OMTN, Volume *23*

Supplemental Information

AGO-accessible anticancer siRNAs designed with synergistic miRNA-like activity

Dowoon Gu, Seung Hyun Ahn, Sangkyeong Eom, Hye-Sook Lee, Juyoung Ham, Dong Ha Lee, You Kyung Cho, Yongjun Koh, Elizaveta Ignatova, Eun-Sook Jang, and Sung Wook Chi

Table S1

Table S1. Sequences of miRNAs used in this study. “m” denotes 2’-O methyl modification. “Ø” indicates abasic deoxynucleotide (dSpacer). “(dT)” represented thymidine deoxynucleotide. All RNAs were synthesized with 5’ phosphate (5’p). Of note, miR-1-5p was synthesized to harbor one more nucleotide in 3’ end in addition to the annotated sequence in miRBase (MI0000651) in order to have two nucleotide 3’ overhang as an optimized form.

Name	Description	Sequences
NT (MI0000038)	Guide Passenger	5’p UCACAØCCUCCUAGAAAGA (dT)(dT) 3’ 5’p UCUUUØUAGGAGGUUGUGA (dT)(dT) 3’
miR-1 (MI0000651)	5p 3p	5’p ACAUACUUCUUUAUAUGCCCAUA 3’ 5’p UGGAAUGUAAAGAAGUAUGUAU 3’
miR-206 (MI000490)	5p 3p	5’p ACAUGCUUCUUUAUAUCCCCAUA 3’ 5’p UGGAAUGUAAGGAAGUGUGUGG 3’
miR-329 (MI0001725)	5p 3p	5’p GAGGUUUUCUGGGUUUCUGUUUC 3’ 5’p AACACACCUGGUUAACCUCUUU 3’
miR-376a (MI0000784)	5p 3p	5’p GUAGAUUCUCCUUCUAUGAGUA 3’ 5’p AUCAUAGAGGAAAAUCCACGU 3’
miR-218 (MI0000294)	Guide Passenger	5’p UUGUGCUUGAUCUAACCAUGU 3’ 5’p mAmUGGUUAGAUCAAGCACAA(dT)(dT) 3’
miR-497 (MI0003138)	Guide Passenger	5’p CAGCAGCACACUGUGGUUUGU 3’ 5’p mAmAACCACAGUGUGCUGCUG(dT)(dT) 3’

Table S2

Table S2. Sequences of siRNAs used in this study. “m” denotes 2’-O methyl modification. “(dT)” represented thymidine deoxynucleotide. All RNAs were synthesized with 5’ phosphate (5’p)..

Sequences of siRNAs used in this study

Name	Description	Sequences
E6	Guide	5’p AUCAGGUAGCUUGUAGGGU(dT)(dT) 3’
	Passenger	5’p ACCCUACAAGCUACCUGAU(dT)(dT) 3’
206/E7	Guide	5’p UGGAAUGCUCGAAGGUCGU(dT)(dT) 3’
	Passenger	5’p ACGACCUUCGAGCAUUCCA(dT)(dT) 3’
206/Her2	Guide	5’p UGGAAUGUAUACCGGCCCU(dT)(dT) 3’
	Passenger	5’p AGGGCCGGUAAACAUUCCA(dT)(dT) 3’
206/EphA2	Guide	5’p UGGAAUGUUUGACACCCUC(dT)(dT) 3’
	Passenger	5’p GAGGGUGUCAAACAUUCCA(dT)(dT) 3’
218/E7	Guide	5’p UUGUGCUUGCCAGAAUCUU(dT)(dT) 3’
	Passenger	5’p mAmAGAUUCUGGCAAGCACAA(dT)(dT) 3’
497/E6	Guide	5’p CAGCAGCACGAAUGGCACU(dT)(dT) 3’
	Passenger	5’p mAmGUGCCAUUCGUGCUGCUG(dT)(dT) 3’

Table S3

Table S3. Base pairs between miRNAs and target sites identified in Figure 1C.

```
miR-497          5′-CAGCAGCACACUGUGGUUUGU-3′
497/E6-1         5′-CAGCAGCAUGGGGUAUACU(dT)(dT)-3′
                    |||||||||||||||||
Reference genome 3′-UACGUCGUACCCCAUAUGA-5′ (278-297)
E6/E7 transcript 3′----------------------5′
```

```
miR-497          5′-CAGCAGCACACUGUGGUUUGU-3′
497/E6-2         5′-CAGCAGCACGAAUGGCACU(dT)(dT)-3′
                    |||||||||||||||||
Reference genome 3′-AACGUCGUGCUUACCGUGA-5′ (513-532)
E6/E7 transcript 3′-AACGUCGUGCUUACCGUGA-5′ (308-327)
```

```
miR-376a         5′-AUCAUAGAGGAAAAUCCACGU-3′
376/E7           5′-AUCAUAGAAGGUCAACCGG(dT)(dT)-3′
                    |||||||||||||||||
Reference genome 3′-CUGUAUCUUCCAGUUGGCC-5′ (652-671)
E6/E7 transcript 3′-CUGUAUCUUCCAGUUGGCC-5′ (447-466)
```

```
miR-1            5′-UGGAAUGUAAAGAAGUAUGUAU-3′
miR-206          5′-UGGAAUGUAAGGAAGUGUGUGG-3′
206/E7           5′-UGGAAUGCUCGAAGGUCGU(dT)(dT)-3′
                    |||||||||||||||||
Reference genome 3′-ACCUUACGAGCUUCCAGCAGA-5′ (830-849)
E6/E7 transcript 3′-ACCUUACGAGCUUCCAGCAGA-5′ (625-644)
```

```
miR-329          5′-AACACACCUGGUUAACCUCUUU-3′
329/E7-1         5′-AACACACAAAGGACAGGGU(dT)(dT)-3′
                    ||||||||||||||||||
Reference genome 3′-CUGUGUGUUUCCUGUCCCA-5′ (865-884)
E6/E7 transcript 3′-CUGUGUGUUUCCUGUCCCA-5′ (660-679)
```

```
miR-329          5′-AACACACCUGGUUAACCUCUUU-3′
329/E7-2         5′-AACACACCACGGACACACAA(dT)(dT)-3′
                    ||||||||||||||||||
Reference genome 3′-ACGUGUGGUGCCUGUGUGU-5′ (876-895)
E6/E7 transcript 3′-ACGUGUGGUGCCUGUGUGU-5′ (671-690)
```

```
miR-218          5′-UUGUGCUUGAUCUAACCAUGU-3′
218/E7-1         5′-UUGUGCUGUCUCUAGCUCU(dT)(dT)-3′
                    ||||||||||||||||||
Reference genome 3′-GACACGACAGAGAUCGAGA-5′ (1095-1114)
```

```
miR-218          5′-UUGUGCUUGAUCUAACCAUGU-3′
218/E7-2         5′-UUGUGCUUGCCAGAAUCUU(dT)(dT)-3′
                    ||||||||||||||||||
E6/E7 transcript 3′-CACACGAACGGUCUUAGAA-5′ (926-945)
```

```
miR-218          5′-UUGUGCUUGAUCUAACCAUGU-3′
218/E7-3         5′-UUGUGCUGCCUCCUGCAAA(dT)(dT)-3′
                    ||||||||||||||||||
Reference genome 3′-GACACGACGGAGGACGUUU-5′ (1177-1196)
```

Table S4

Table S4. Oligonucleotides used for qPCR in this study.

Gene	Direction	Sequences
E6	Forward	5’ GCGACCCTACAAGCTACCTG 3’
	Reverse	5’ GCACTGGCCTCTATAGTGCC 3’
E7	Forward	5’ GCTGAACCACAACGTCACAC 3’
	Reverse	5’ CACGGACACACAAAGGACAG 3’
PTK9	Forward	5’ CCCAAGGATTCAGCTCGTTA 3’
	Reverse	5’ GCAGTCAACTCATCCCCATT 3’
ADAR1	Forward	5’ CCCTTCAGCCACATCCTTC 3’
	Reverse	5’ GCCATCTGCTTTGCCACTT 3’
SSRP1	Forward	5’ TGACTACAAGATCCCCTACACC 3’
	Reverse	5’ GAGTTTGGCCTTGCTTGATTG 3’
ROBO1	Forward	5’ CTTACACCCGTAAAAGTGACGC 3’
	Reverse	5’ TGGTCTCTCTAAGACAGTCAGC 3’
EphA2	Forward	5’ TGGCTCACACACCCGTATG 3’
	Reverse	5’ GTCGCCAGACATCACGTTG 3’
Her2	Forward	5’ TGCAGGGAAACCTGGAACTC 3’
	Reverse	5’ ACAGGGGTGGTATTGTTCAGC 3’
GAPDH	Forward	5’ TGCACCACCAACTGCTTAGC 3’
	Reverse	5’ GGCATGGACTGTGGTCATGA 3’

Figure S1

A

Sample name	AGO CLIP read	Mapped (HPV18 reference)	Overlap Read (BC≥2)
HeLa-A-2A8	10,802,378	1,707	7,654
HeLa-B-2A8	11,104,169	3,006	
HeLa-A-7G1-1	12,204,108	2,307	
HeLa-B-7G1-1	12,957,786	1,322	

Sample name	AGO CLIP read	Mapped (E6/E7 HeLa)	Overlap Read (BC≥2)
HeLa-A-2A8	10,802,378	1,328	4,344
HeLa-B-2A8	11,104,169	1,483	
HeLa-A-7G1-1	12,204,108	945	
HeLa-B-7G1-1	12,957,786	660	

B

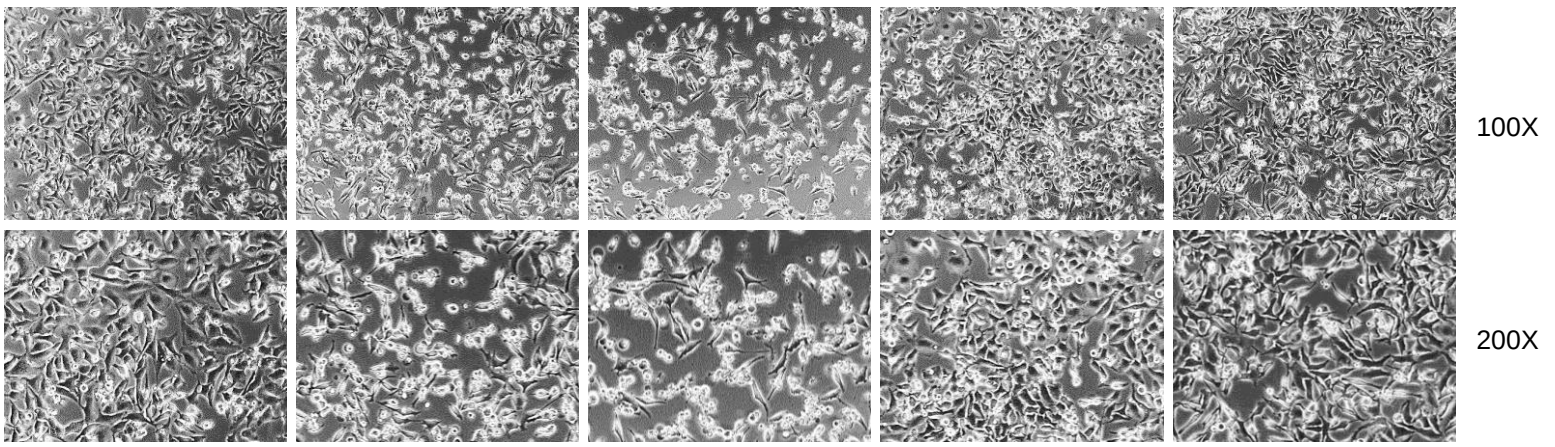

C

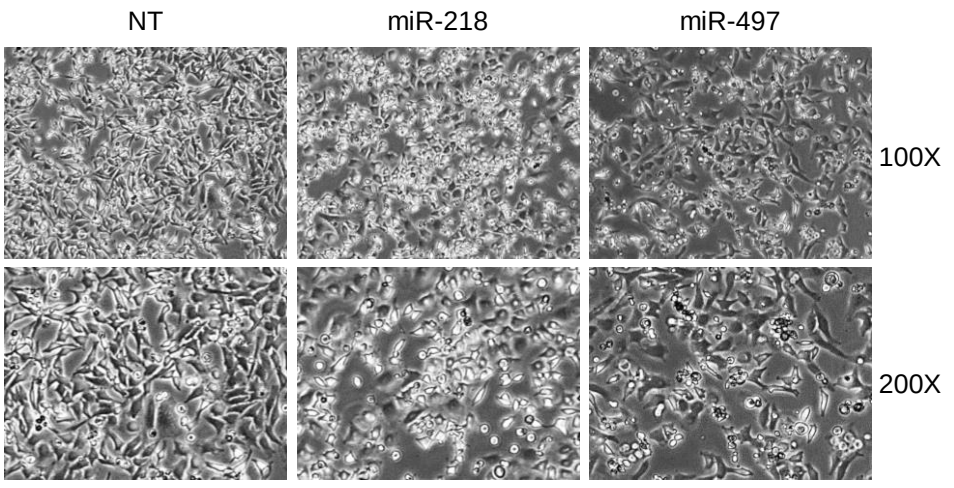

Figure S1. AGO CLIP analyses for HPV18 transcripts identify putative antitumor miRNAs in cervical cancer cell HeLa. **(A)** AGO CLIP reads, independently derived from replicate experiments in HeLa (n=2; A and B) with two different antibodies (2A8 and 7G1-1)[1], were mapped on HPV18 reference genome (NC_001357; left panel) or E6/E7 transcript identified in HeLa (M20324; right panel), ultimately selecting reproducible AGO-bound regions in HPV18 based on overlaps of reads from different antibodies (biological complexity; BC≥2). **(B-C)** HeLa cells after 48 hours from the transfection of non-targeting control (NT), miR-1, miR-206, miR-329 and miR-376a (B) or NT, miR-218 and miR-497 (C). 2 times magnified pictures at the same time point were displayed in lower panel.

Figure S2

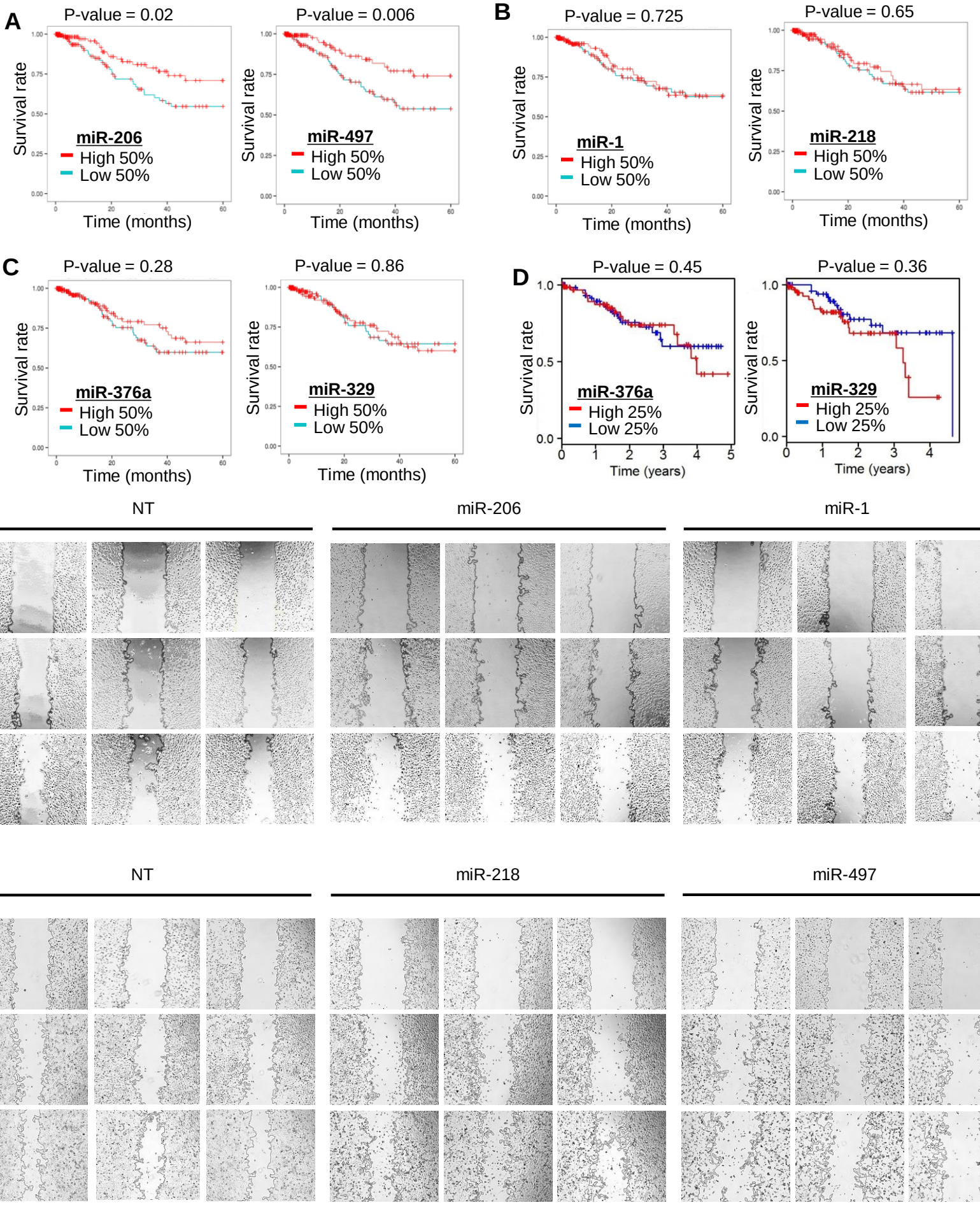

Figure S2. Survival analyses and wound-healing assays for miR-1, miR-206, miR-218 and miR-497. (A-C) Survival analyses of cervical cancer patients compared in split-half according to expression of given miRNAs (high 50% vs. low 50%); miR-206 and miR-497 (A); miR-1 and miR-218 (B); miR-376a and miR-329 (C); P-value, log-rank test; 5-year survival rate. Notably, all the split-half analysis results were derived from the previous report[2]. (D) Survival analysis for the highest quartile (high 25%) vs. lowest quartile (low 25%) was also performed for miR-376a and miR-329. Of note, there is no significant difference from miR-376a and miR-329 expression; P-value, log-rank test; 5-year survival rate. **(D-E)** Bright field images of wound healing assays in HeLa performed for the expression of NT, miR-206 and miR-1 (D); NT, miR-218 and miR-497 (E).

Figure S3

A

Sample name	Cell	Transfection	Total read	Mapped read (RefSeq)	%
HeLa-NT	HeLa	NT	8,124,115	7,517,279	93
HeLa-206	HeLa	miR-206	9,610,463	9,056,493	94
HeLa-206/E7	HeLa	206/E7	9,031,012	8,684,546	96
HeLa-E6	HeLa	E6 siRNA	8,672,277	8,260,161	95
HeLa-218	HeLa	miR-218	7,594,575	6,437,221	85
HeLa-218/E7	HeLa	218/E7	9,401,240	8,103,785	86
HeLa-497	HeLa	miR-497	8,206,381	6,994,613	85
HeLa-497/E7	HeLa	497/E7	9,910,971	7,550,507	76

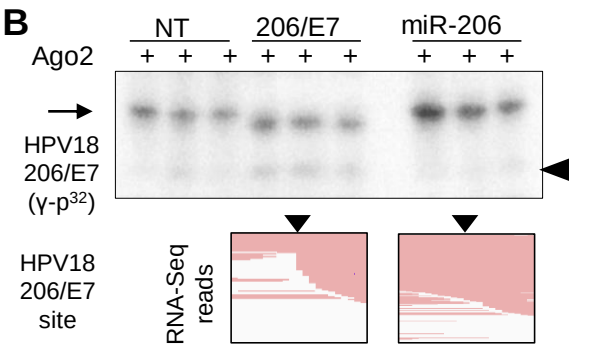

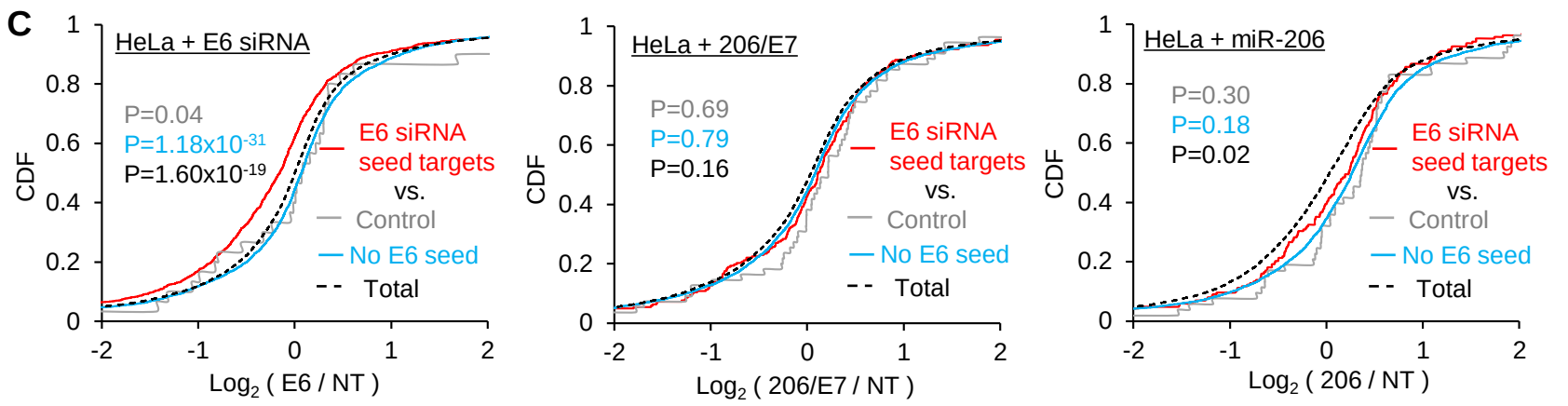

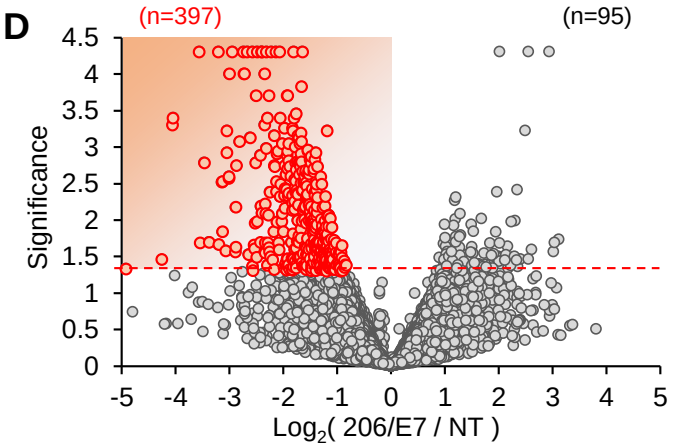

F

Category	Term	EASE score
KEGG_PATHWAY	Purine metabolism	6.83 x 10^{-5}
KEGG_PATHWAY	Biosynthesis of antibiotics	0.0066
KEGG_PATHWAY	RNA transport	0.0117
KEGG_PATHWAY	Cell cycle	0.0169
BIOCARTA	RB Tumor Suppressor/Checkpoint Signaling in response to DNA damage	0.0172
KEGG_PATHWAY	Pentose phosphate pathway	0.0222
BIOCARTA	p53 Signaling Pathway	0.0289

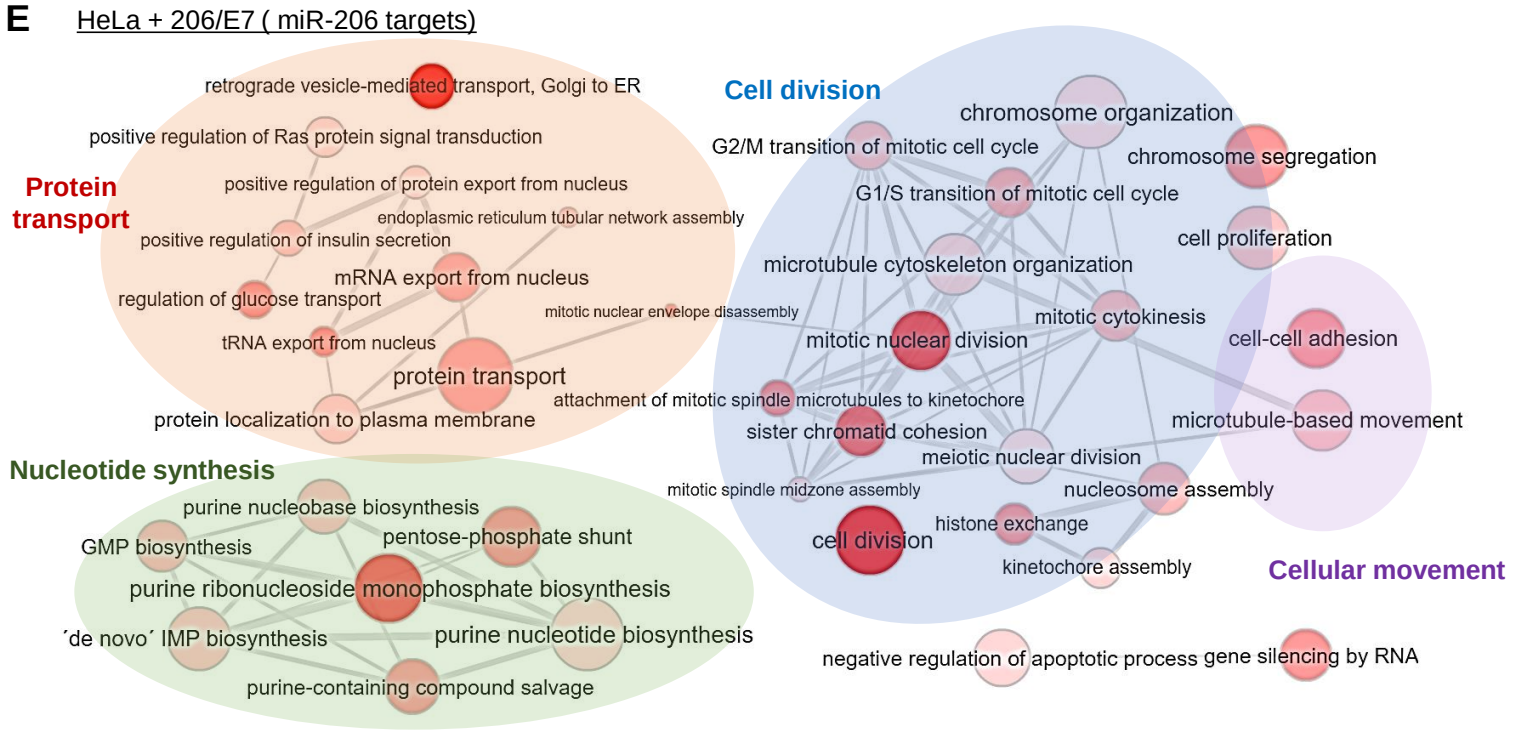

Figure S3. Effect of 206/E7 expression on transcriptome of cervical cancer HeLa. **(A)** Mapping rates of RNA-Seq reads obtained after transfection of given siRNA, miRNA or mi/siRNA into HeLa; TopHat2 results with RefSeq annotation. **(B)** *in vitro* Ago2 cleavage assays performed for 206/E7, comparing with the control siRNA (NT) and miR-206 (upper panel); black arrow, the expected size of cleavage product. RNA-Seq reads aligned in the target sites were also displayed for 206/E7 and miR-206 expression (lower panel); black arrows, position of the expected cleavage site. **(C)** CDF analyses of putative E6 siRNA seed targets (red line), of which 3'UTRs contain E6 seed sites, in the presence of E6 siRNA (left panel), 206/E7 (middle panel) or miR-206 (right panel) as conducted in Figure 4B; RPKM values from StringTie; P-values from KS test, two-sided; grey, relative to transcript with control site (control)[3]; cyan, relative to transcripts with no E6 seed site (no E6 seed); black, relative to total transcript (total). **(D)** The volcano plot analysis to select downregulated DEG (red dots, $P < 0.05$; Cuffdiff) depending on 206/E7 expression in HeLa; significance, $-\log_{10}$(P-value). **(E)** GO analysis results of miR-206 targets, of which 3'UTRs harbor miR-206 seed sites in the identified downregulated DEG (206/E7 transfected HeLa; C), displayed as networks of enriched biological processes (EASE score < 0.2, DAVID; node size and color intensity inversely correlate with P-value). **(F)** Pathways from KEGG and BIOCARTA database, significantly enriched ($P < 0.05$; DAVID) in miR-206 targets of downregulated DEG in the presence of 206/E7.

Figure S4

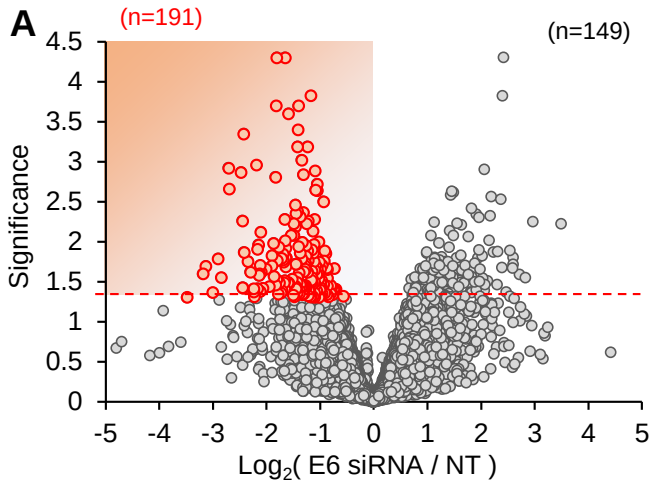

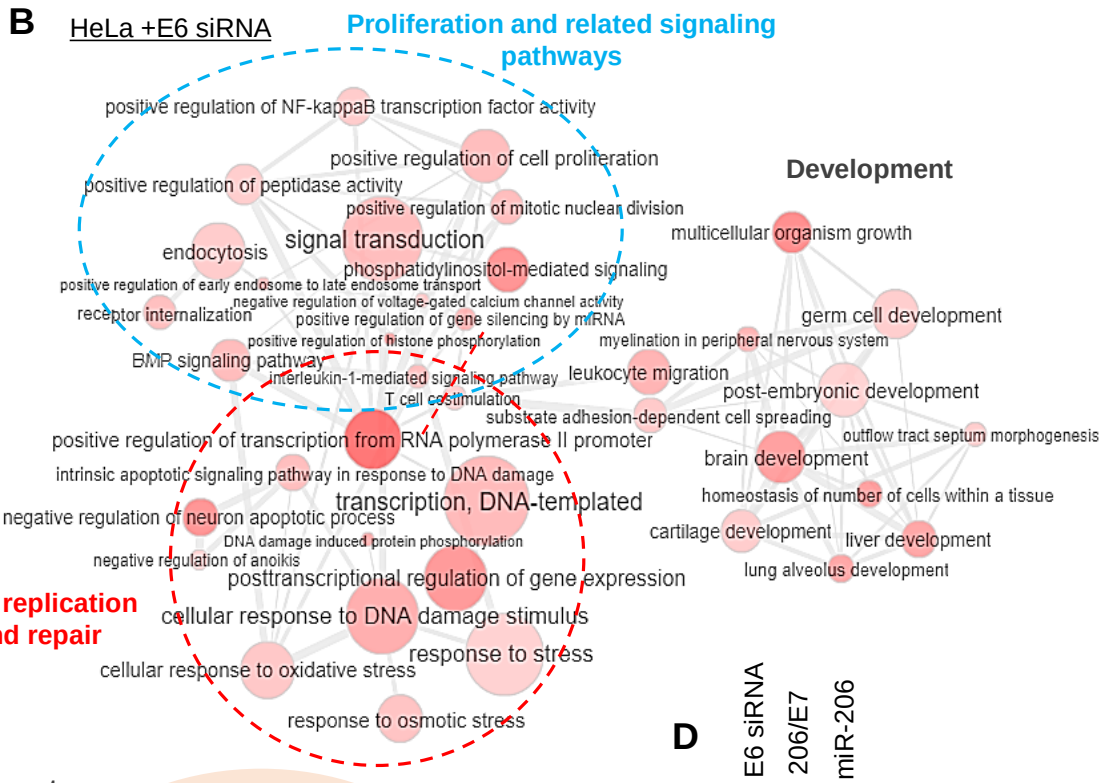

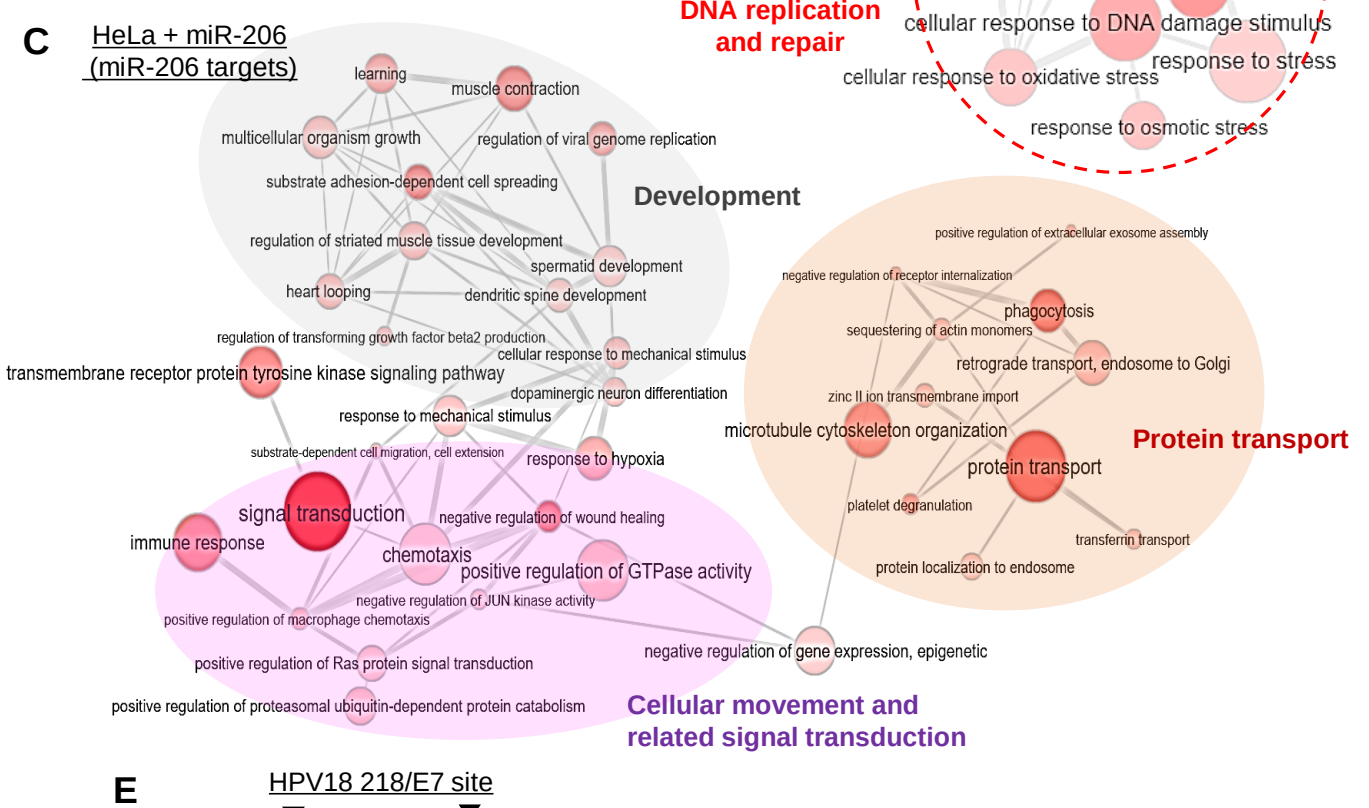

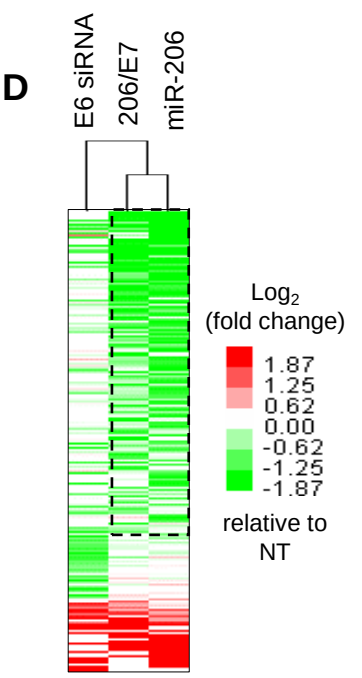

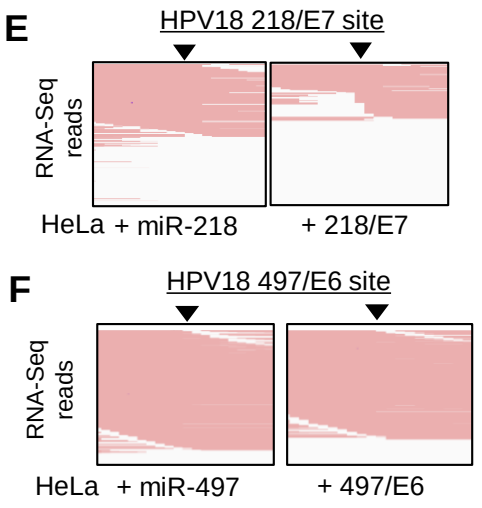

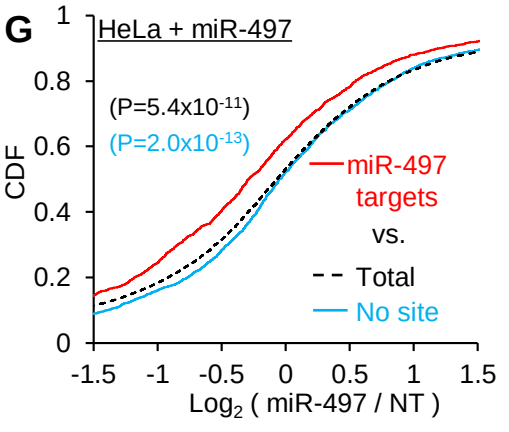

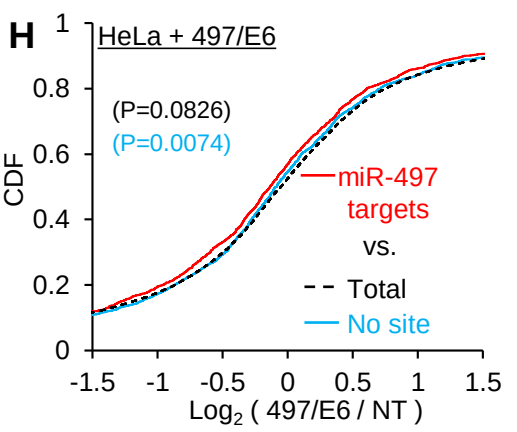

Figure S4. Transcriptome-wide analysis of E6 siRNA and miR-206 in HeLa. **(A)** Transcriptome profiles of E6 siRNAs analyzed by the volcano plot analysis; significance, -$\log_{10}$(P-value); downregulated DEG (red dots; dotted line, $P < 0.05$; Cuffdiff). Of note, similar numbers of DEG in both downregulation and upregulation were observed (n=191 vs. 149) when putative off-targets, which contain a seed site of E6 siRNA (6mer; position 2-7) in 3'UTRs, were not accounted. **(B)** GO analysis results of downregulated DEG in E6 siRNA transfected HeLa. Enriched biological processes were displayed as networks (EASE score < 0.15, DAVID; node size and color intensity inversely correlate with P-value). Notably, only clusters of graphs with high connection were displayed. **(C)** Same GO analysis as performed in (B) except for miR-206 targets in miR-206 transfected HeLa with EASE score < 0.2. Of note, due to the marginal effect of miR-206 on the silencing of E6/E7 transcript (only 20% reduction), expression of miR-206 could be used to delineate the effect of miR-206-like activity for 206/E7 on transcriptome and its regulatory function for tumor. **(D)** Hierarchical cluster analyses for the putative miR-206 target transcripts in DEGs ($P<0.01$; Cuffdiff) in the presence of miR-206, 206/E7 and E6 siRNA, represented as a heatmap. Of note, the largest cluster in the negative $\log_2$ fold change (relative to control; NT) was identified between miR-206 and 206/E7 (dotted rectangle), indicating that 206/E7 exerts miR-206-like repression at transcriptome-wide level. **(E)** RNA-Seq reads aligned in the HPV18 218/E7 target site are displayed for miR-218 and 218/E7 expression; black arrows, position of the expected cleavage site. Notably, only 218/E7 showed the cleavage pattern of the target site. **(F)** Same analyses as in (E) except for miR-497 and 497/E6. **(G-H)** CDF analyses of miR-497 targets (red line), which harbor seed sites in 3'UTRs, in miR-497 (D) or 497/E6 transfected HeLa; P-values from KS test, two-sided; black, relative to total transcript (total); cyan, relative to transcripts with no miR-498 seed site (no site). Of note, RPKM values were derived from Cuffdiff ($P<0.1$).

Figure S5

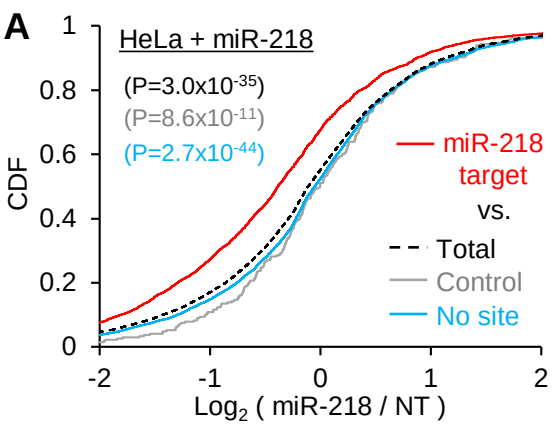

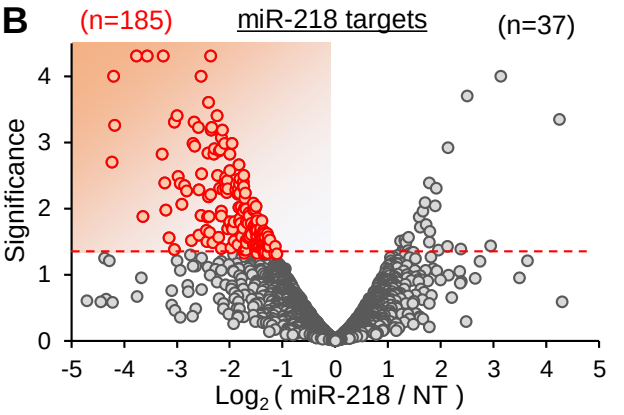

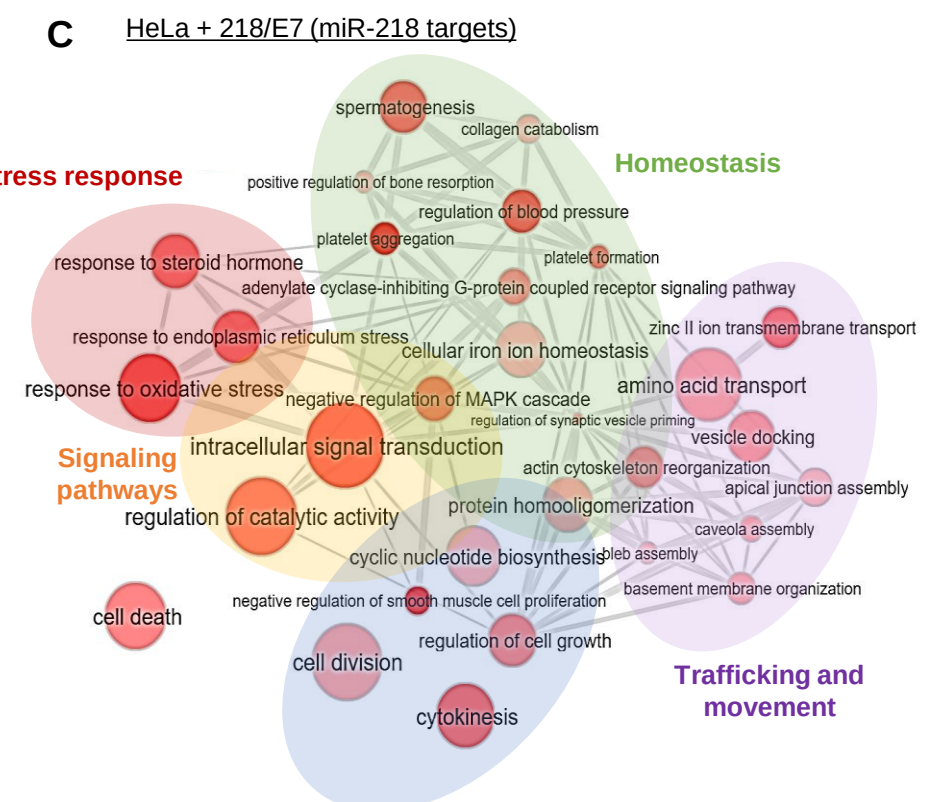

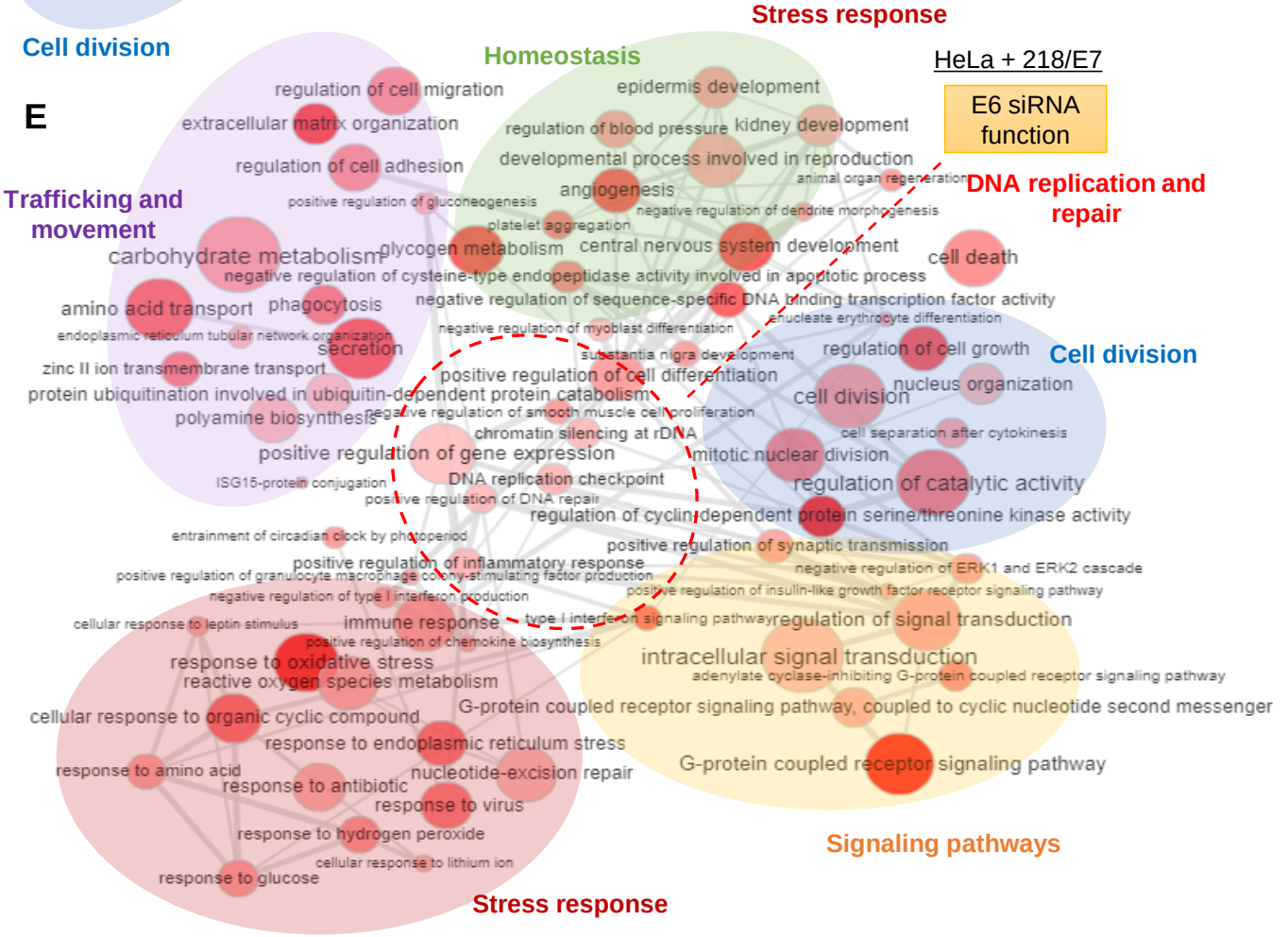

Figure S5. Global effect of 218/E7 transfection on transcriptome of cervical cancer HeLa. (A-B) CDF (A) or volcano plot (B) analyses of miR-218 targets, of which 3'UTRs contain seed sites, in miR-218 transfected HeLa; RPKM values were derived from cufflinks (A) or Cuffdiff (B). P-values were from KS test, two-sided (A); red line, miR-218 targets; black dotted line, relative to total transcript (total); grey line, relative to transcript with control site (control) (3) ; cyan line, relative to transcripts with no miR-218 seed site (no site). Downregulated DEG were represented in red ($P < 0.05$, Cuffdiff; B). **(C-D)** GO analyses of biological processes for miR-218 targets of downregulated DEG in 218/E7 transfected (C) or miR-218 transfected HeLa (D); EASE score < 0.2, DAVID; node size and color intensity inversely correlate with P-value. **(E)** Same GO analysis as in (C-D) except for downregulated DEG in 218/E7 transfected HeLa.

Figure S6

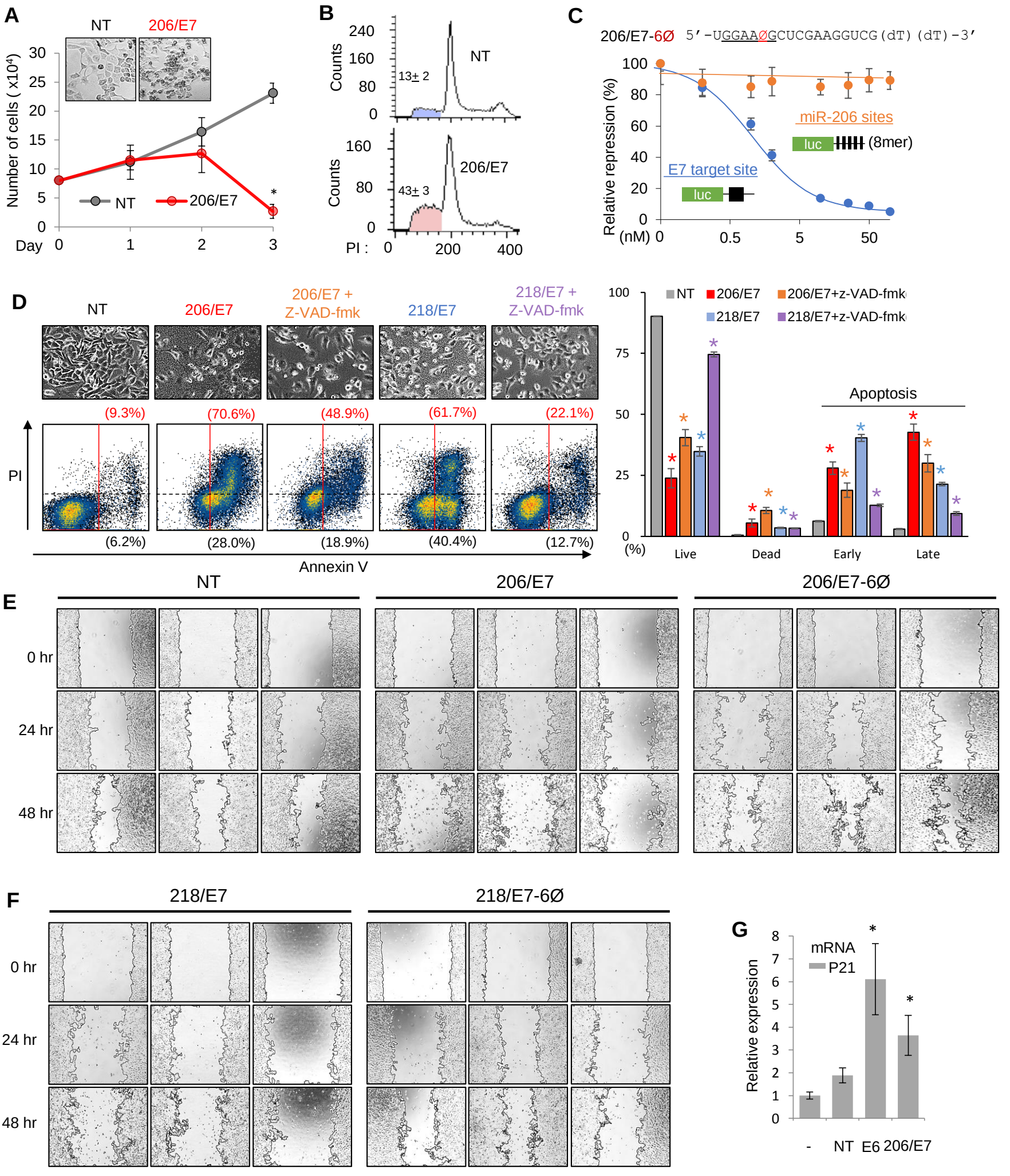

Figure S6. Effect of 206/E7 and 218/E7 on cervical cancer HeLa. (A) Quantitation of live cells after transfection of 206/E7 into HeLa cells; cell images (upper inset). **(B)** Propidium iodide (PI) staining results of 206/E7 transfected HeLa, of which sub G1 population was observed to be increased, indicating induction of apoptotic DNA fragmentation; measured by flow cytometry. **(C)** Abasic pivot substitution (dSpacer in position 6; 6Ø) applied to the 206/E7 sequence (upper panel). Luciferase reporter assays with E7 target site and miR-206 seed sites were performed for 206/E7-6Ø under different concentrations (lower panel). Of note, 206/E7-6Ø lost miRNA-like activity that could suppress miR-206 seed sites but maintain on-target activity for silencing the E7 target site. For this reason, siRNA activity and miRNA activity could be separately distinguished from 206/E7 activity by using 6Ø modification. **(D)** Same cell death analysis performed in Figure 5A except including 20μM Z-VAD-fmk treatment; flow cytometry results from PI and Annexin V staining (left panel); quantitation results (right panel). **(E-F)** Would healing assays of NT, 206/E7 and 206/E7-6Ø transfected (E) or 218/E7 and 218/E7-6Ø (F) transfected HeLa. All replicate images are shown with lines, drawn for quantitation in Figure 5C-D by using ImageJ program. **(G)** Abundance of P21 mRNA in 206/E7 transfected HeLa, compared with E6 siRNA transfection; qPCR measurement, relative expression normalized by GAPDH mRNA. All P-values were from t-test, two-sided; *, $P < 0.05$; relative to non-targeting control, NT; n = 3; repeated with biologically independent samples; graphs, mean; error bars, SD; otherwise indicated.

Figure S7

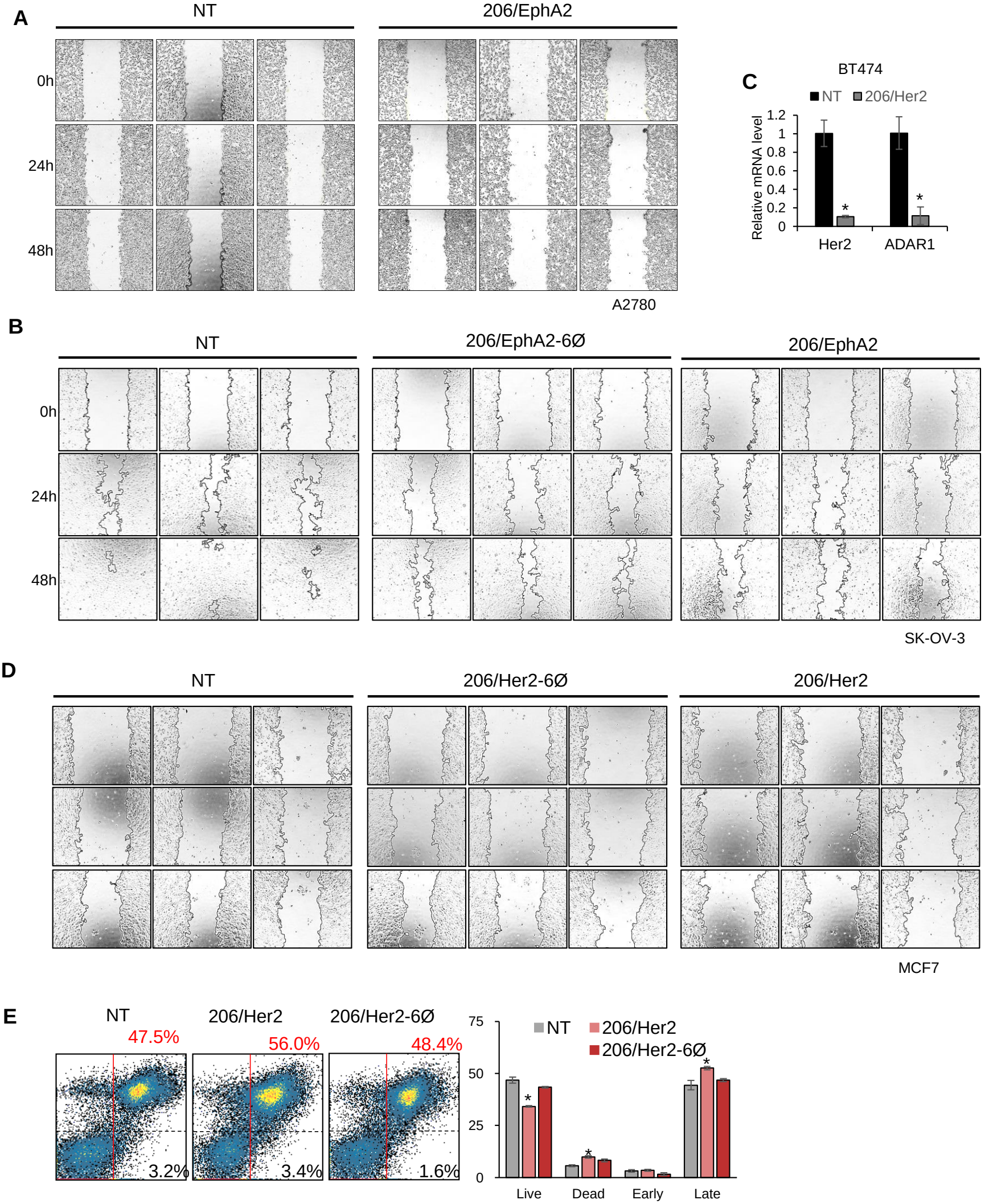

Figure S7. Experimental validation of antitumor mi/siRNAs designed for ovarian and breast cancer. **(A)** Wound healing assays of 206/EphA2 transfected ovarian cancer cell A2780. **(B)** Same wound healing assay in (A) except transfecting 206/EphA2-6Ø into SK-OV-3 cells. **(C)** Effect of 206/Her2 on expression of on-target (Her2) and miR-206 target (ADAR1) mRNAs, measured by qPCR in breast cancer cell BT474; *, P < 0.05; t-test, two-sided; relative to non-targeting control, NT; n=3; repeated with biologically independent samples; graphs, mean; error bars, SD. **(D)** Wound healing assays for 206/Her2 and 206/EphA2-6Ø in breast cancer cell MCF7. **(E)** Cell death assays of NT, 206/Her2 or 206/Her2-6Ø transfected MCF7; flow cytometry (left panel) and its quantitative results (right panel) as conducted in Figure 1E–F. Of note, increased basal cell death in MCF7 cells was likely due to using a different batch, comparing with one used in Figure 7I-L; *, P < 0.05; t-test, two-sided; relative to non-targeting control, NT; n=3; repeated with biologically independent samples; graphs, mean; error bars, SD.

REFERENCES

1. Chi, S.W., Zang, J.B., Mele, A. and Darnell, R.B. (2009) Argonaute HITS-CLIP decodes microRNA-mRNA interaction maps. *Nature*, **460**, 479-486.

2. Chung, I.F., Chang, S.J., Chen, C.Y., Liu, S.H., Li, C.Y., Chan, C.H., Shih, C.C. and Cheng, W.C. (2017) YM500v3: a database for small RNA sequencing in human cancer research. *Nucleic Acids Res*, **45**, D925-D931.

3. Chi, S.W., Hannon, G.J. and Darnell, R.B. (2012) An alternative mode of microRNA target recognition. *Nat Struct Mol Biol*, **19**, 321-327.